Available online at www.sciencedirect.com
ScienceDirect
Journal of Hazardous Materials 150 (2008) 300–307
Journal of Hazardous Materials
www.elsevier.com/locate/jhazmat

Oxidation and isomerization of cyclohexane catalyzed by SO_4^{2-}/Fe_2O_3-CoO under mild condition

Hongwei Chen, Bo Wang *, Hongzhu Ma, Xue Cui

Key Laboratory of Applied Surface and Colloid Chemistry, Ministry of Education, Institute of Energy-Chemistry, School of Chemistry and Materials Science, Shaanxi Normal University, 710062 Xi'An, PR China

Received 14 December 2006; received in revised form 19 April 2007; accepted 19 April 2007
Available online 24 April 2007

Abstract

SO_4^{2-}/Fe_2O_3-CoO solid catalyst was prepared and characterized by X-ray diffraction (XRD), scanning electron microscope (SEM) and Fourier transfer infrared (FT-IR) spectroscopy. Its catalytic activities in oxidation and isomerization of cyclohexane in air under mild condition were studied by UV, GC/MS and XPS. The results suggested that isomerization and oxidation of cyclohexane under mild conditions can synchronously performed and the catalytic activity of the catalyst can be improved by promotion of Co element into the sulfated iron. The high catalytic activities of catalysts may be related to the shift of the asymmetric stretching frequency of the S=O bonds of sulfate species. Finally, the possible mechanism was also proposed.

Keywords: Isomerization; Oxidation; Cyclohexane; SO_4^{2-}/Fe_2O_3-CoO

1. Introduction

The oxidation of cyclohexane is an important reaction in the framework of commercial production of nylon [1]. Past studies have revealed that the main products formed during its oxidation are cyclohexanol, cyclohexanone, adipic acid and several minor products (cyclohexene, cyclohexan-2-one, valeraldehyde and valeric acid) [2]. Many studies have been made to develop new catalysts to oxidize cyclohexane under mild conditions with high selectivity for the target products (cyclohexanol, cyclohexanone or adipic acid) using different oxidizing agents (hydrogen peroxide, *t*-butyl hydroperoxide and molecular oxygen) [3]. A recent paper has investigated $Co(II)V(IV)L^{2+}$ as catalyst oxidized cyclohexane to cyclohexanone and cyclohexanol in the ratio of 14:1 [4].

Acid catalysts play an important role in organic synthesis and transformations. Many organic reactions such as alkylation, isomerization, esterification, and rearrangements can be catalyzed by acid catalysts. The occurrence of oxidative dehydrogenation of cyclohexane to cyclohexene and benzene on MoO_3 or Mo/r-Al_2O_3 catalyst in the temperature range 553–690 K has been reported [5]. Selectivity to dehydrogenated products is influenced by side-reactions such as combustion or cracking, leading to a heavy selectivity decrease at increasing temperature. A paper reported that high temperature production of benzene from cyclohexane in vapor phase over several catalysts; such as V_2O_5/TiO_2, Ce-, V-, Fe-phosphates, H-ZSM5 [6]. Ciambelli [7] found that cyclohexane can be selectively oxidized to benzene on $MoOx/TiO_2$ catalyst in the presence of gaseous oxygen at temperature of 308 K under UV illumination.

To better understand some fundamental aspects of isomerization and oxidation of cyclohexane, in this paper, SO_4^{2-}/Fe_2O_3-CoO solid superacid was prepared and its catalytic properties in isomerization and oxidation reaction of cyclohexane in air under mild condition were also studied. Former papers usually reported isomerization or oxidative dehydrogenation, here, however, SO_4^{2-}/Fe_2O_3-CoO as a catalyst synchronously performed isomerization and oxidative dehydrogenation under mild conditions.

* Corresponding author. Tel.: +86 29 85308442; fax: +86 29 85307774.
E-mail address: wangbo@snnu.edu.cn (B. Wang).

0304-3894/$ – see front matter © 2007 Elsevier B.V. All rights reserved.
doi:10.1016/j.jhazmat.2007.04.101

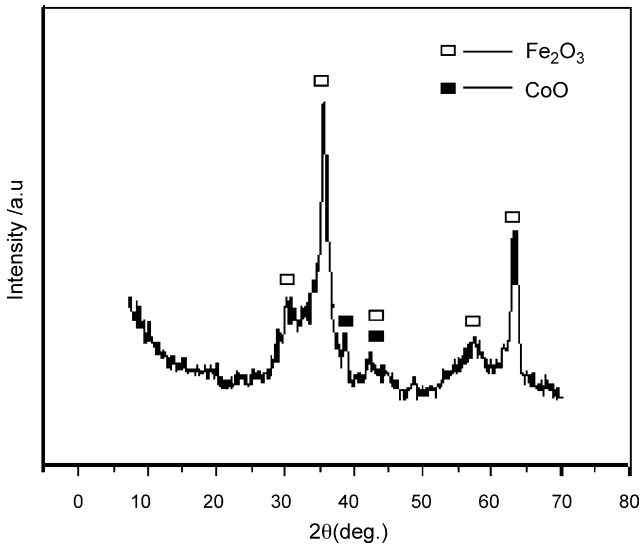

Fig. 1. XRD patterns of SO_4^{2-}/Fe_2O_3-CoO catalyst.

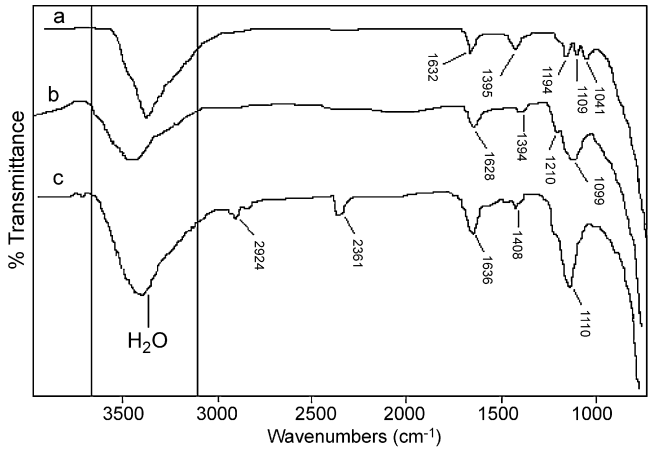

Fig. 3. FT-IR spectra of different catalyst, [(a) SO_4^{2-}/Fe_2O_3-CoO catalyst before reaction; (b)SO_4^{2-}/Fe_2O_3 catalyst before reaction; (c)SO_4^{2-}/Fe_2O_3-CoO after reaction].

2. Experimental

2.1. Catalyst preparation

$Fe_2(SO_4)_3$ and $CoCl_2$ were mixed according to approximately 1% Fe(wt.%), 0.5 %Co(wt.%) and dissolved in distilled water, followed by adding 25%$NH_3{\cdot}H_2O$ dropwise with stirring; final pH of solution was adjusted to 8–9. The obtained precipitate was washed several times with deionized water until no Cl^- detected in the filtrate, and then dried at 383 K to obtain CoO/Fe_2O_3. To prepare SO_4^{2-}/Fe_2O_3-CoO, CoO/Fe_2O_3 was placed on a glass suction funnel, covered with 0.5 mol/L H_2SO_4, and allowed to stand for 12 h. After the sample was filtered and dried, it was calcined in air at 823 K for 3 h and stored in a sealed glass ampoule for use.

2.2. Catalyst characterization

X-ray diffractograms (XRD) were obtained in a Rigaku apparatus using Cu Kα radiation (λ = 1.5406 Å). The XRD phases present in the samples were identified with help of JCPDS data files.

The surface composition of the catalyst was analyzed by X-ray photoelectron spectroscopy (XPS) using a XSAM800 (Kratos) equipment operated in FAT mode with non-monochromatic Mg X-radiation ($h\nu = 1253.6$ eV). The base pressure in the chamber was in the range of 10^{-8} Pa. Charging of catalyst sample was corrected by setting the binding energy of adventitious carbon(C 1s) at 284.6 eV. The samples were out gassed in a vacuum oven overnight before XPS measurements. The specific area data (BET/N_2 method) were determined on Micromeritics ST-08 equipment using N_2 as the adsorbent.

Fourier transform infrared (FT-IR) spectra were obtained in a heatable gas cell at room temperature using a Bruker model EQUINX55 spectrometer. The samples were heated under vacuum at 373–773 K for 1 h before recording spectra. FT-IR spectra of 1% (wt.%) catalyst in KBr disk were obtained in the range 4000–400 cm^{-1}.

The scanning electron microscope (SEM) measurements were performed using Quanta 200 scanning electron microscope produced by Philips at 20 kV.

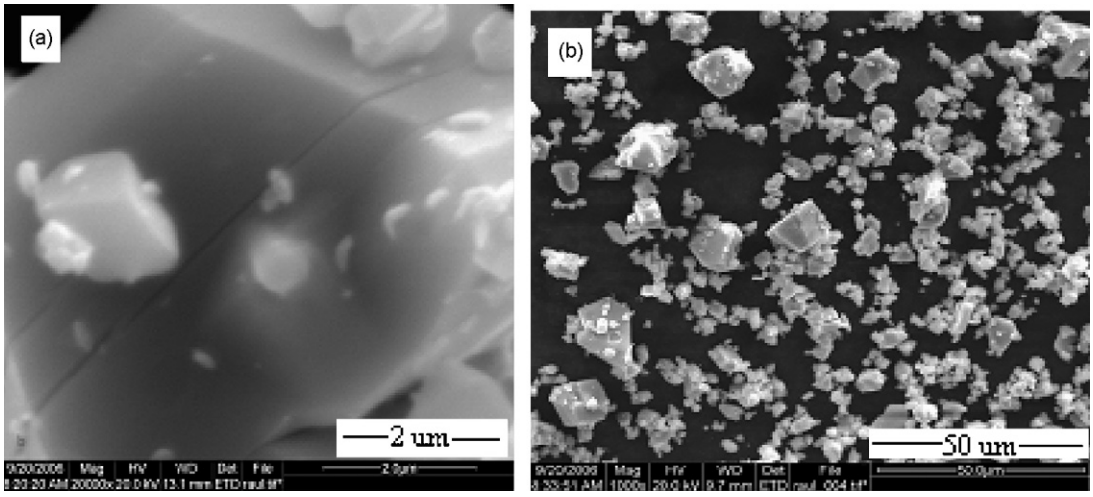

Fig. 2. SEM micrographs of SO_4^{2-}/Fe_2O_3-CoO fresh catalyst: (a) ×20,000; (b) ×1000.

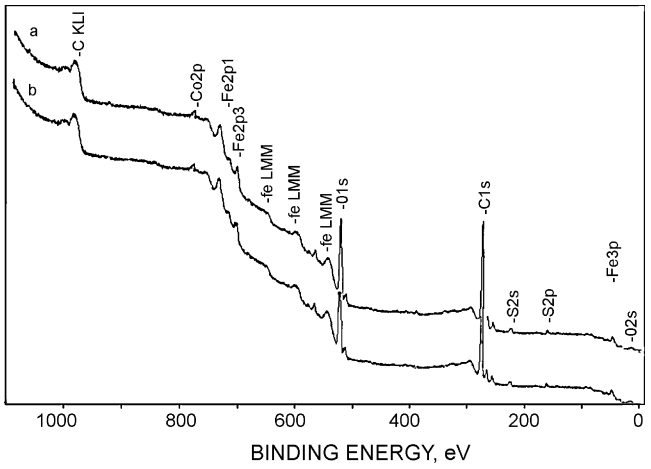

Fig. 4. XPS spectra of SO_4^{2-}/Fe_2O_3-CoO catalyst before (a) and after (b) reaction.

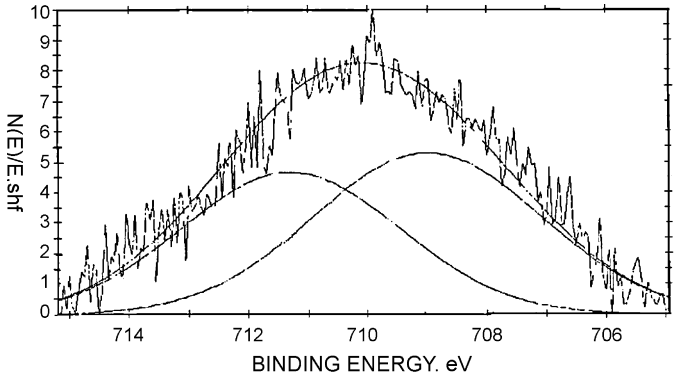

Fig. 5. XPS pattern of used catalyst Fe 2p.

2.3. Reaction tests and product analysis

Catalytic tests were carried out under atmospheric pressure in a continuous flow fixed bed quartz reactor. Before exposure to reactant, the modified solid catalyst underwent gradual heating under nitrogen in temperature-ramped mode up to 773 K and maintained for 30 min, then cooled to 303 K under nitrogen and kept at this temperature during reaction. Then cyclohexane and air was introduced into the reactor with a condenser to prevent the volatilization of the reactant. Generally, 5 g of catalyst and 120 ml cyclohexane was used for each experiment, unless stated otherwise. The total volumetric flow rate of air was 1 m^3/min. Reaction products and the intermediates were analyzed by on-line with UV spectroscopy and GC/MS using a Hewlett-packard 5985 B quadrupole mass spectrometer and an RTE-IV data system.

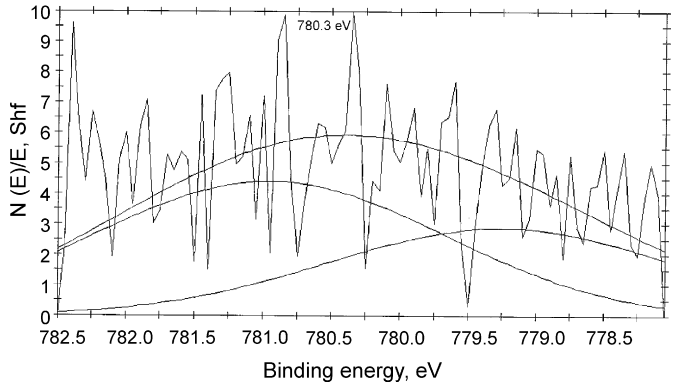

Fig. 6. XPS pattern of used catalyst Co2p.

3. Results and discussion

3.1. Crystalline structure of the catalyst

Fig. 1 represents XRD patterns of the samples calcined at 550 °C. Several peaks at 30.2°, 35.4°, 42.3°, 57.2° and 63.4° of 2θ were observed, which correspond to {2 2 0}, {1 1 0}, {3 1 1}, {0 2 4}, {2 1 4} of Fe_2O_3, respectively [8]. Two peaks at 36.5° and 42.3° can be assigned to CoO crystal scattering from {1 1 1} and {2 0 0} planes, respectively [9], indicating the amorphous CoO and Fe_2O_3 transformed to crystallite CoO and Fe_2O_3 at 550 °C for about 3 h.

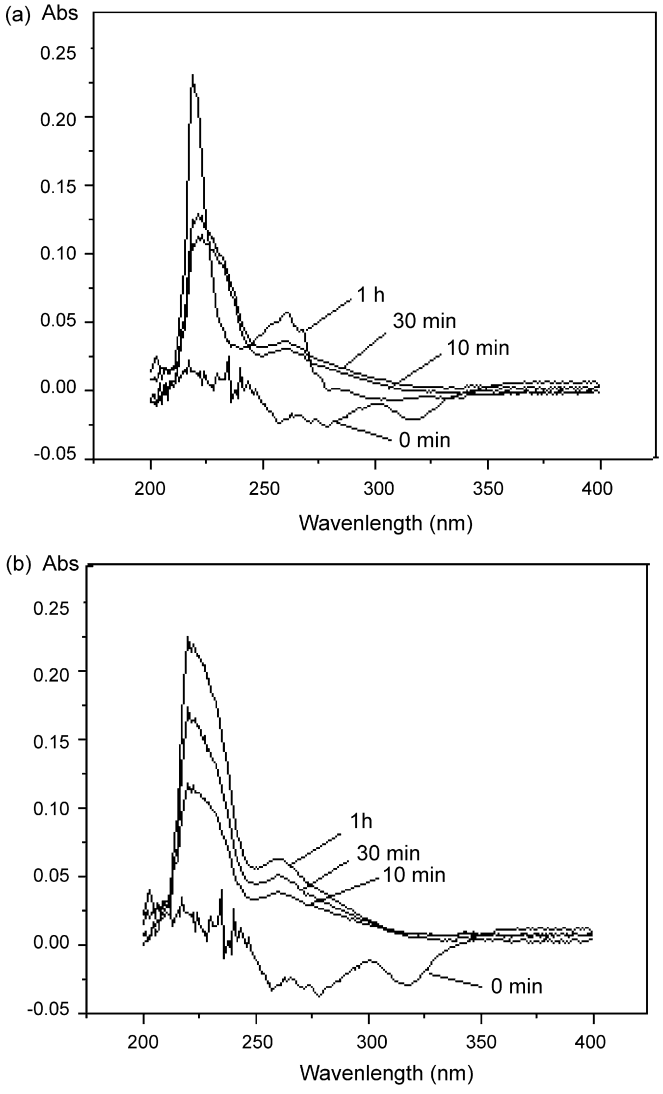

Fig. 7. UV spectra for cyclohexane reaction system with different catalyst [(a) SO_4^{2-}/Fe_2O_3-CoO and (b) SO_4^{2-}/Fe_2O_3].

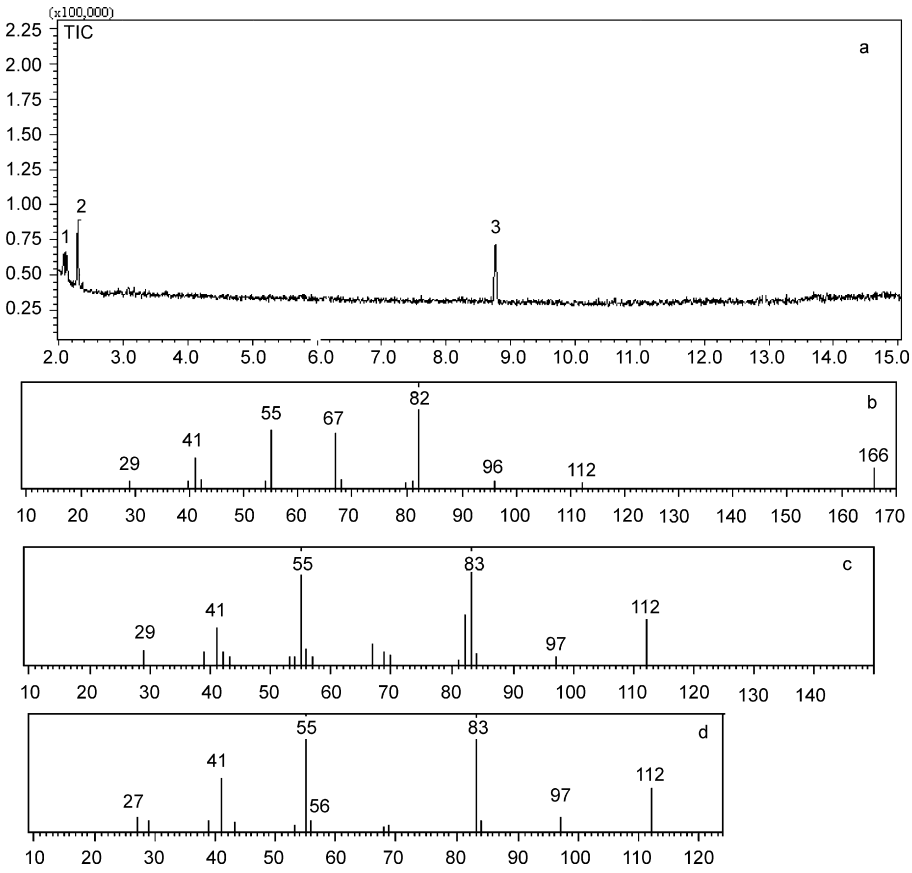

Fig. 8. GC/MS analysis of products 10 min later: (a) TIC of products, (b) 1st peak of TCL, (c) 2nd peak of TCL, (d) 3rd peak of TCL.

The different morphologies of SO_4^{2-}/Fe_2O_3-CoO catalyst in different scales are shown in Fig. 2. Fig. 2(a) clearly shows the presence of large octahedral crystals with a 8 μm diameter particle and there are many small particles on the surface of the granule. Fig. 2(b) clearly shows the catalyst has regular nano grains and would not congregate, which indicates the catalyst can fully contact with the reaction mass.

The specific surface areas of SO_4^{2-}/Fe_2O_3 and modified SO_4^{2-}/Fe_2O_3-CoO catalyst measure by the BET/N_2 method were about 82 $m^2\ g^{-1}$, indicated that the catalyst has the higher special surface area, and it would be benefit to the improvement of the catalyst activity.

3.2. FT-IR spectra of the catalyst

FT-IR spectra of SO_4^{2-}/Fe_2O_3-CoO, SO_4^{2-}/Fe_2O_3 before reaction and after reaction are given in Fig. 3. In general, when metal oxides were modified with sulfate ion followed by evacuating above 400 °C, a strong band assigned to S=O stretching frequency was observed at 1360–1410 cm^{-1} [10–15]. In Fig. 3(a), a sharp band at 1395 cm^{-1} correspond to S=O asymmetric stretching frequency of sulfate ion accompanying by three broad, split band at 900–1200 cm^{-1} was observed, indicating that the presence of two kinds of sulfated species. The tiptop vibrancy peak of sulfated radicals was above 1200 cm^{-1}, indicating that the Lewis acid strength of Fe^{3+} becomes stronger, which maybe due to CoO coordinated to the S=O groups that acts as electron withdrawing species followed by the inductive effect, this results are in agreement with reference reported [16]. In comparison with Fig. 3(a), the weak absorption of Fig. 3(b) at 1041 cm^{-1} completely disappear, indicating modified CoO change the configuration of sulfated Fe_2O_3. The split band at 900–1200 cm^{-1} disappears for SO_4^{2-}/Fe_2O_3-CoO after reaction (Fig. 3(c)), indicating Lewis acid sites disappear after reaction.

3.3. XPS analysis

The XPS survey spectra of SO_4^{2-}/Fe_2O_3-CoO catalyst before and after reaction are shown in Fig. 4. The binding energy of sulfur S 2p was observed at 168.4 eV, which suggested that sulfur in the catalyst existed in a six-oxidation state (S^{6+}). It is an important sign to indicate the formation of the superacid. After the reaction, the binding energies of S 2p almost unchanged, inferring that the valence of S were unchanged, it may be concluded that the catalyst can be reused and the catalytic activity was almost unchanged.

XPS Fe 2p3/2 peak of solid superacid catalyst after catalytic reaction is shown in Fig. 5 and it can be found that XPS Fe 2p3/2 peak has been deconvoluted to two different binding energies of 711.3 eV and 709.0 eV assigned to two valent components Fe^{3+} and Fe^{2+}, respectively, the ratio of two atoms is 45.71:54.29 (molar ratio), inferred that iron was the mixture of Fe^{2+} and Fe^{3+} in the catalyst after reaction, which

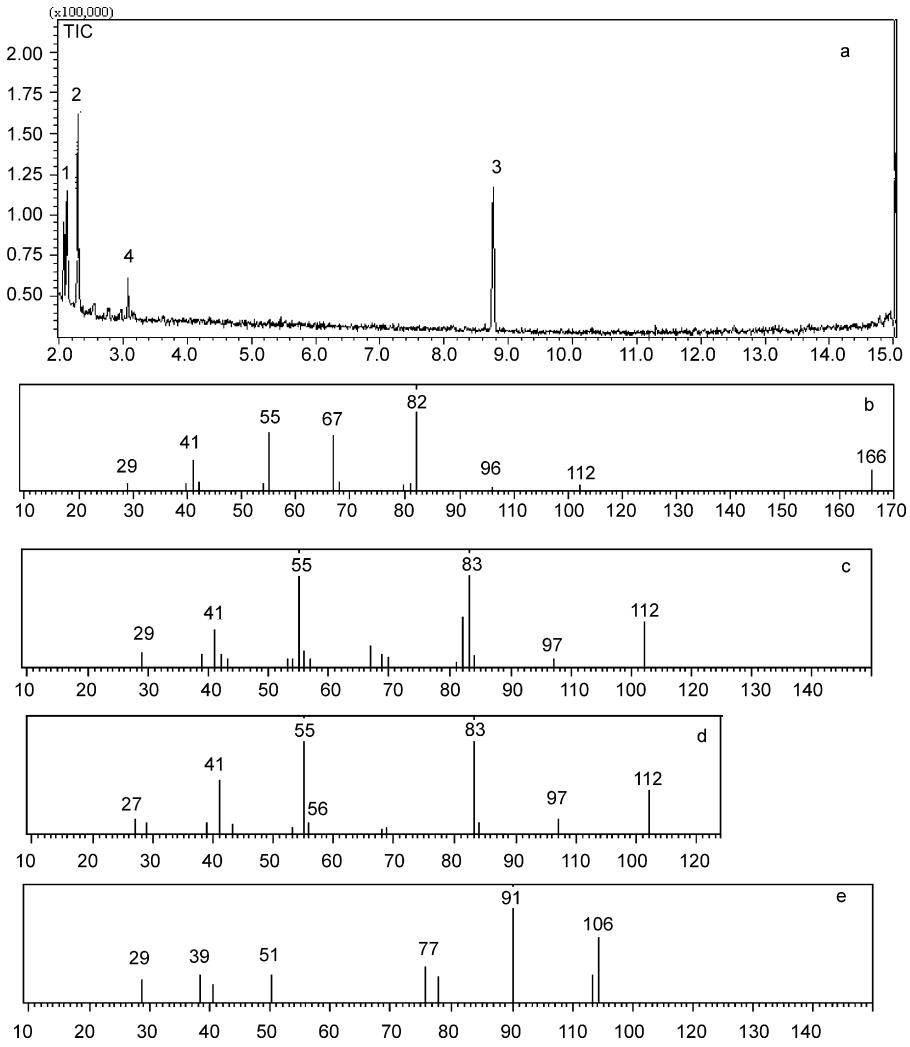

Fig. 9. GC/MS analysis of products 1 h later: (a) TIC of products, (b) 1st peak of TCL, (c) 2nd peak of TCL, (d) 3rd peak of TCL, (e) 4th peak of TCL.

illuminated that Fe^{3+} was reduced to Fe^{2+} during the reaction process.

In Fig. 6, the divalent cobalt form (Co^{2+}) accounted for 60.42% of the total elemental cobalt and the trivalent cobalt form (Co^{3+}) occupied 39.58%. In comparison to the Co^{2+}, which occupied 100% of the total cobalt element before the reaction, this finding illuminated the fact that the CoO was involved with the reaction and was oxidized to Co_2O_3.

3.4. Catalytic reaction and product analysis

In order to demonstrate that catalyst and the oxygen were necessary for the oxidation, at first the reaction was carried out without the catalyst or air for as long as 12 h at room temperature and no product were detected. Then the catalyst was introduced into the reactor and a strong smell at the end of the oxidation reaction was detected, indicating the formation of the product and the influence of the catalyst and the oxygen, which is further confirmed by the GC/MS and UV analysis.

UV spectra of cyclohexane samples with different catalysts and various times in the range of 400–200 nm was shown in Fig. 7. With the reaction proceeding, two absorption bands at 222 and 265 nm were observed. While the characteristic absorption band of benzene ring at 265 nm was almost invisible in the first 1 h, indicating that no aromatic compound has been formed in the initial product, until 1 h later the characteristic absorption bands of benzene ring was observed when SO_4^{2-}/Fe_2O_3-CoO was used as the catalyst (Fig. 7(a)), which was also confirmed by GC/MS. But for unmodified SO_4^{2-}/Fe_2O_3 reaction system, the B absorption band of benzene ring at 265 nm was almost invisible even 1 h later, indicating no aromatic compound was produced, and may be conclude that introduction of cobalt in the SO_4^{2-}/Fe_2O_3 catalyst can promote the aromatization of cyclohexane.

To further confirm the process, the product distribution in 10 min and 60 min was taken for GC/MS analysis and the results show in Figs. 8 and 9 (the peak of the reactant was taken off). It can be found that three products which were produced after 10 min with retention time at 8.767, 2.292, 2.125 min were detected in Fig. 8(a). The corresponding mass spectra were listed in Fig. 8(b)–(d), which clearly confirmed the formation of dicyclohexane, ethylcyclohexane and 2.4-dimethyl-2-hexene,

Table 1
Catalytic performance of cyclohexane over SO_4^{2-}/Fe_2O_3-CoO catalyst

Time (min)	Cyclohexane conversion (%)	Product selectivity (%)			
		Dicyclohexane	Ethycyclohexane	2,4-Dimethl-2-hexane	Ethylbenzene
10	29.21	59.09	40.91	34.09	
60	60.41	24.47	35.11	26.60	13.82

Reaction condition: $T = 303$ K; air pressure.

respectively. Fig. 9(a) shows four peaks at retention time 8.767, 3.075, 2.292, 2.125 min, indicating four products assigned to dicyclohexane, ethylcyclohexane and 2,4-dimethyl-2-hexene, ethylbenzene, respectively (Fig. 9(b)–(e)) were produced 1 h later. Product selectivity and conversion of cyclohexane were summarized in Table 1.

3.5. Reaction mechanism

Because ethylbenzene was not found in the products at the first 10 min, which probably illustrated that ethylcyclohexane was converted into ethylbenzene from oxidative dehydrogenation. Some researches have proved the probability that ethylcyclohexane can be converted into ethylbenzene [6]. So the possible mechanism of the oxidation of cyclohexane in air in presence of SO_4^{2-}/Fe_2O_3-CoO was proposed and may occur through two steps as follows:

3.5.1. Step 1: isomerization reaction

The overall reaction mechanism of the isomerization of cyclohexane over SO_4^{2-}/Fe_2O_3-CoO was considered. The paper showed the monomolecular reaction proceeded on the Lewis acid sites [13].

In the given mechanism, the catalyst behaves as a typical Lewis acid in an oxidation reaction [14]. In this, it forms an anion radical through an electron abstractor, which can add an oxygen molecule as shown in Scheme 1: firstly, oxygen combined with the superacidic Lewis acid sites generated a complex iron(III) peroxide species. The complex cation attacked to RH(cyclohexane) generated a key intermediates. The products were cyclohexanol or cyclohexanone when Lewis acid sites and oxygen molecule bonds cleaved [15,16]. In our experiment, however, C–C bonds and C–O bonds of cyclohexane cleaved, so the products did not discover cyclohexanol or cyclohexanone.

The significant intermediate performed two different pathways: Pathway a performed C–O bonds cleaved and generated cyclohexane carbenium ion. Pathway b performed cleavage of C–C bonds and mainly generated ethyl carbenium ion and *n*-butane carbenium ion. In the reaction process, performance of catalyst was possibly cata-$FeOO^+$ captured H^- from cyclohexane and then performed two possible pathways: pathway 1 escape H^- regenerated catalytic activity, however, pathway 2 obtained H^- lose catalytic activity. In the process, iron(III) was reduced to iron(II), this result was also proved by XPS spectra. In the pathway a, cyclohexane carbenium ion reacted with cyclohexane and generated dicyclohexane. In the pathway b,

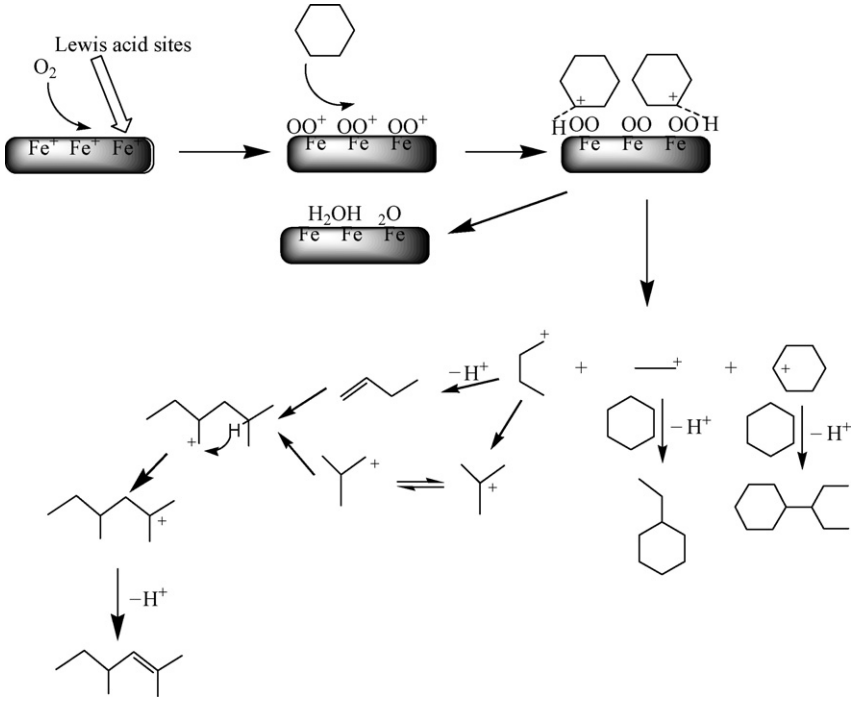

Scheme 1. Possible mechanism of isomerization of cyclohexane catalyzed by SO_4^{2-}/Fe_2O_3-CoO.

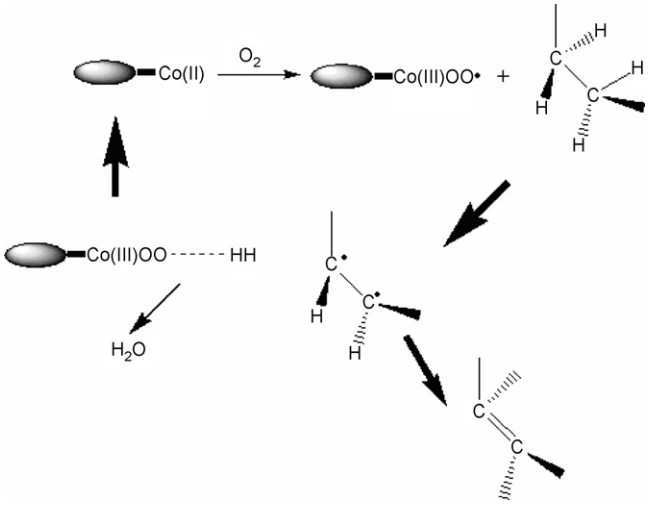

Scheme 2. Possible mechanism of oxidation of SO_4^{2-}/Fe_2O_3-CoO.

ethyl carbenium ion combined with cyclohexane to result in the formation of ethylcyclohexane. For *n*-butane carbenium ion, however, the branching step necessitates formation of the primary isobutyl cation [17]. It was proved that the intermediate species is a *t*-butyl cation formed on the superacidic Lewis site by abstraction of a H^- from isobutene, followed by the alkylation with butane to form trimethylpentanes (TMP) as shown in Scheme 1 [18]. Accordingly, the reaction is alkylation of alkenes with isobutene via the t-butyl cation formed on highly superacidic sites to result in the formation of TMP. The reaction has so far been considered to be the alkylation of isobutene with alkenes via the protonated alkenes as an intermediate. The mechanism of the formation of 4-dimethyl-2-hexene was shown in Scheme 1.

3.5.2. Step 2: oxidative dehydrogenation

We thought the occurrence of oxidative dehydrogenation of ethylcyclohexane to ethylbenzene on Co(II) in this step. A recent paper investigated the production of benzene from cyclohexane in vapor phase over Co-ZSM5 [6]. This result has also been proved by the former paper [5]. The process of oxidative dehydrogenation was shown in Scheme 2. In the process, Co(II) obtained O_2 firstly was oxidized and secondly was reduced. It was proved that the value of Co was changed by XPS. The paper investigated catalysis mechanism for oxidative dehydrogenation over cobalt-based catalysts [19].

Based on the above discussions it can be concluded that the isomerization of annular alkanes over solid superacids proceeded by the monomolecular mechanism on the Lewis acid sites in the induction period. Later, the occurrence of oxidative dehydrogenation of ethycyclohexane in mild conditions, with high selectivity to ethylbenzene, has been observed on Co-supported solid superacid.

4. Conclusion

SO_4^{2-}/Fe_2O_3-CoO solid superacid catalyst was synthesized. The product was analyzed by UV and GC/MS. Its catalytic properties in the isomerization and oxidation of cyclohexane in air under mild condition were studied by UV, GC/MS and XPS. The results suggested that isomerization and oxidation of cyclohexane under mild conditions can synchronously performed and the catalytic activity of the catalyst can be achieved by promotion of Co element into the sulfated iron. The high catalytic activities of catalysts may be related to the shift of the asymmetric stretching frequency of the S=O bonds of sulfate species. Finally, the possible mechanism was also proposed.

References

[1] H. Arakawa, M. Aresta, J.N. Armor, M.A. Beckman, A.T. Bell, J.E. Bercaw, C. Creutz, E. Dinjus, D.A. Dixon, K. Domen, D.L. DuBois, J. Eckert, E. Fujita, D.H. Gibson, W.A. Goddard, D. Wayne, Goodman, J. Keller, G.J. Kubas, H.H. Kung, J.E. Lyons, L.E. Manzer, T.J. Marks, K. Morokuma, K.M. Nicholas, R. Periana, L. Que, J.R. Nielson, W.M.H. Sachtler, L.D. Schmidt, A. Sen, G.A. Somorjai, P.C. Stair, B. Ray Stults, Catalysis research of relevance to carbon management: progress, challenges, and opportunities, Chem. Rev. 101 (2001) 953–967.

[2] N. Perkas, Y. Holypin, O. Patalik, A. Gedonken, S. Chandrasekhran, Oxidation of cyclohexane with nanostructured amorphous catalysts under mild conditions, Appl. Catal. A: Gen. 209 (2001) 125–130.

[3] C.B. Almquist, P. Biswas, The photo-oxidation of cyclohexane on titanium dioxide: an investigation of competitive adsorption and its effects on product formation and selectivity, Appl. Catal. A: Gen. 214 (2001) 259–271.

[4] M. Jhansi, L. Kishore, G.S. Mishra, AnilKumar, Synthesis of hetero binuclear macrocyclic Co–V complex bonded to chemically modified alumina support for oxidation of cyclohexane using oxygen, J. Mol. Catal A: Chem. 230 (2005) 35–42.

[5] E.C. Alyea, M.A. Keane, The oxidative dehydrogenation of cyclohexane and cyclohexene over unsupported and supported molybdena catalysts prepared by metal oxide vapor deposition, J. Catal. 164 (1996) 28–35.

[6] M. Panizza, C. Resini, G. Busca, E.F. Lopez, V.S. Esccribano, Selective catalytic reduction of NO_x by methane over Co-H-MFI and Co-H-FER zeolite catalysts: characterisation and catalytic activity, Catal. Lett. 89 (2003) 1–4.

[7] P. Ciambelli, G. Lisanti, D. Sannino, V. Palma, The TPCAT4 Pre-Conference Symposium in Kobe- Catalysis for the Environment and New Energy Sources, Kobe, Japan, July 12, 2002.

[8] X. Wang, L. Gao, H. Zheng, M. Ji, T. Shen, Z. Zhang, Fabrication and electrochemical properties of α-Fe_2O_3 nanoparticles, J. Crys. Growth 269 (2004) 489–492.

[9] Y. Ye, F. Yuan, S. Li, Synthesis of CoO nanoparticles by esterification reaction under solvothermal conditions, Mater. Lett. 60 (2006) 3175–3178.

[10] J.R. Sohn, J.G. Kin, T.V. Kwon, E.H. Park, Measurement of the thermal properties of gadolinium and dysprosium titanate, Langmuir 18 (2002) 1666–1676.

[11] O. Sanur, M. Bensitel, A.B.M. Saad, J.C. Cavallcy, C.P. Tripp, B.A. Morrow, The structure and stability of sulfated alumina and titania, J. Catal. 99 (1986) 104–110.

[12] T. Yamaguchi, Recent progress in solid superacid, Appl. Catal. 61 (1990) 1–11.

[13] H Matsuhashi, H Shibata, H Nakamura, K Arata, Skeletal isomerization mechanism of alkanes over solid superacid of sulfated zirconia, Appl. Catal. A: Gen. 187 (1999) 99–106.

[14] A. Corma, H. Garcia, Naphthalene included within all-silica zeolites: influence of the host on the naphthalene photophysics, Chem. Rev. 102 (2002) 3837–3849.

[15] B. Moden, Bi-ZengZhan, J. Dakka, J.G. Santiesteban, E. IgIesia, Kinetics and mechanism of cyclohexane oxidation on MnAPO-5 catalysts, J. Catal. 239 (2006) 390–401.

[16] P. Du, J.A. Moulijn, G. Mul, Selective photo(catalytic)-oxidation of cyclohexane: effect of wavelength and TiO_2 structure on product yields, J. Catal. 238 (2006) 342–352.

[17] J. Sommer, R. Jost, M. Hachoumy, Activation of small alkanes on strong solid acids: mechanistic approaches, Catal. Today. 38 (1997) 309–319.
[18] K. Arata, H.M. Hino, H. Nakamura, Synthesis of solid superacids and their activities for reactions of alkanes, Catal. Today 81 (2003) 17–30.
[19] B. Han, Z. Liu, Q. Liu, L. Yang, Z-L. Liu, W. Yu, An efficient aerobic oxidative aromatization of Hantzsch 1,4-dihydropyridines and 1,3,5-trisubstituted pyrazolines, Tetrahedron Lett. 62 (2006) 2492–2496.